ECO (E)

abstract *The effective resonance integral and the Doppler effect in UO_2 coated particle fuels in a 1/E neutron spectrum were measured by the activation technique, following irradiation of test elements in a fuel vacant position on the core center of the D_2O moderated ECO critical facility. The experimental results obtained here in good agreement with theoretical values calculated by the ZUT-TUZ codes. A semi-empirical formula for the Doppler coefficient β, with range of validity extending over that of the current expressions, was derived and tested for resonance integrals in the range from 12 to 150 b.*

riassunto DETERMINAZIONE SPERIMENTALE DELL'INTEGRALE EFFETTIVO DI RISONANZA E DELL'EFFETTO DOPPLER IN COMBUSTIBILE A BIOSSIDO DI URANIO A PARTICELLE RIVESTITE. *L'integrale effettivo di risonanza e l'effetto Doppler in combustibile costituito da particelle di biossido di uranio rivestite di carbone pirolitico sono stati misurati in uno spettro neutronico 1/E mediante la tecnica di attivazione, irradiando elementi di prova in una posizione vacante del combustibile al centro del nocciolo della struttura critica moderata ad acqua pesante ECO. Sono stati ottenuti risultati sperimentali in buon accordo coi risultati di calcoli teorici effettuati con i codici ZUT-TUZ. Una formula semi-empirica per il coefficiente Doppler β, con intervallo di validità superiore a quelli delle espressioni di uso corrente, è stata derivata e verificata per valori dell'integrale di risonanza compresi tra 12 e 150 b.*

Experimental determination of the effective resonance integral and the Doppler effect for UO_2 coated particle fuel(*)

G. Corbo, L. Haemers, S. Tassan
CCR Euratom, Physics Division - Ispra (Varese)

The article describes a measurement of the effective resonance integral and the Doppler effect for UO_2 coated particle fuels in a 1/E neutron spectrum, and presents a semi-empirical formula derived for the Doppler coefficient β with range of validity extending over that of the current expressions (**).

The purpose of the experiment was the determination of the above parameters over a reasonably extended range of kernel and coating sizes, so as to provide a consistent set of data to check the theoretical treatment of the resonance capture modes typical of granulated fuel (for ex., double heteronegeity). In practice, fuel supply limitations restricted the types of fuel studied to those the characteristics of which are listed in table 1.

In order to avoid useless geometrical complexity, the granulated fuel was vibrocompacted inside a 15 mm diam, 0.3 mm thick, 126 mm high stainless steel tube (test - element). The satisfactory reproducibility of the fuel density in this tube was carefully checked.

The test-element was centered inside a 75 mm diam, 170 mm high, Cd-clad Al container. For the Doppler effect measurement an oven was also placed in the container. It consisted of a 0.5 mm diam. Kanthal *A* wire (resistivity 7.42 Ω/m),

(*) The work described in this paper was performed in the frame of a collaboration agreement between AGIP Nucleare and CCR Euratom Ispra for HTR lattice physics studies.

(**) For a much more detailed report on this work, see ref. [1].

wounded around a pyrophilite tube; thermal insulation was provided by loose quartz wool; the temperature was measured by a chromel-alumel thermocouple inserted in the test-element (fig. 1).

The measurements were performed by the activation technique, irradiating the test-element at a fuel vacant position on the core center of the D_2O moderated ECO critical facility, i.e. in a quasi-$1/E$ spectrum.

For the effective resonance integral experiment, the resonance capture of the test-element was normalized to that of a reference element (chosen as a 19 mm diam UO_2 rod), whose resonance integral is known from previous measurements [2] and can be theoretically calculated with adequate precision. Incidentally, this procedure makes insignificant the effect of small deviations from $1/E$ of the real spectrum, provided that the resonance integrals of the test and reference elements are not too different [3]. For the Doppler effect experiment, two measurements were performed for each fuel type, at 293 °K and 1290 °K respectively.

The measured activities were normalized to the reactor power by reference to the activities induced in Cd-clad, 0.2 mm thick Au foils, placed at a fixed position relative to the test-element.

Either type of experiment supplied results in the form of resonance integral ratios, including the

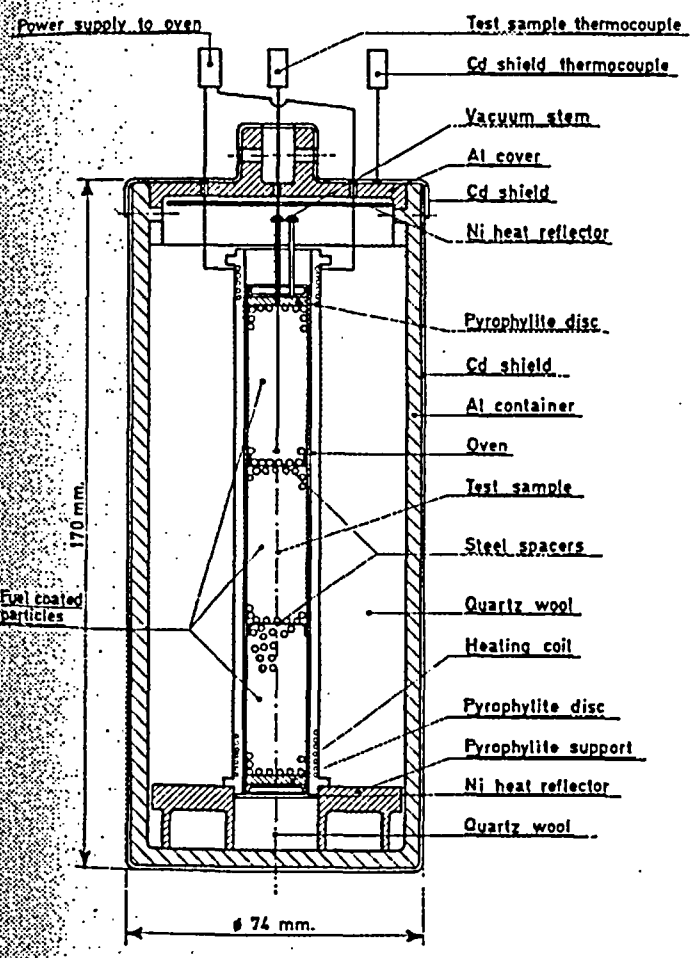

Fig. 1 - The test-element inside its container.

TABLE 1

COATED PARTICLE FUEL CHARACTERISTICS

Fuel identification	Kernel dia. (microns)	Pyrolitic graphite coating thickness (microns)	Homogenized density (g/cm³)	wt % of U
1	773	105	3.69	77.0
2	773	243	2.28	59.3
3	773	377	1.69	44.3
4	514	258	1.91	39.0

TABLE 2

EXPERIMENTAL ERROR ANALYSIS

Error source	σ_R (%)	σ_D (%)
Reproducibility of test-elements	0.7	0.7
Counting samples preparation	0.6	0.6
Counting statistics	0.16	0.16
Self-absorption coefficients in counting	0.03	0.03
Instrumental temperature determination	—	0.03
Variations with temperature in density and void coefficient of test element	—	0.32
Flux normalization	0.1	0.1
Dead time of counting equipment	0.02	0.02
Total error of single measurement	0.92	1.0
Total error of mean of 4 independent measurements	0.46	0.5

so-called 1/v capture contribution. Such (small) contribution was evaluated by a calculation taking into account the moderating effect of the fuel coating graphite [4]. The values of the 1/v capture term so calculated were in the range from 1.31 b (type 1 fuel) to 1.34 b (type 4 fuel).

The sample used for measuring the ^{238}U capture induced activity in the test-element was obtained from the fuel contained in the central 4 cm long segment of the element. This sample consisted of a 3 cc U solution specimen prepared by powderization of the coated kernels, burning of graphite and transformation of UO_2 into U_3O_8, solution in hot HNO_3.

A series of cross-check weight and volume determinations assured the precise knowledge of the U amount in the counting sample.

The induced activity measured was that of ^{239}Np gamma decay. Standard corrections (for ex., for fission products activity) were applied to the counting data [3].

The results of the error analysis carried out for either experiment (resonance integral: σ_R, Doppler effect: σ_D) are presented in condensed form in table 2. Only the not negligible error values are reported. The estimate for the overall experimental error, based on a series of four independent determinations, was typically $\sigma_R = 0.45\%$, $\sigma_D = 0.5\%$. Among the systematic error sources calculated to be insignificant (as also evidenced by ad-hoc auxiliary measurements carried out for previous similar experiments [3, 5]) were: the slight departure of the flux from the $1/E$ dependence at the fuel vacant position where the test-element was inserted, the screening effect of the Ni-Cr wire and the oven materials, the minor heating of the Cd envelope when the test-element was heated to 1290 °K, the approximations in the technique for evaluating the fission products activity correction to the measured counting sample activity.

The results of the effective resonance integral measurement are presented in table 3, as ratios of the « test-element/reference element » values, including the 1/v contribution ($= R_{ex}$). The table contains also the actual experimental error, as inferred in terms of σ from the dispersion of the measured data, as well as the corresponding theoretical values (R_{th}) calculated by the ZUT-TUZ codes [6, 7], and the ANISN code ([4], for the 1/v capture). Table 4 lists the values of the corresponding effective resonance integrals, RI, as inferred from the data of table 3 normalized to a value of 16 b for the resonance integral of the reference rod (Hellstrand [2]), having removed the 1/v capture. The quoted errors derive from the 4% error assigned by Hellstrand to his measurement.

The experimental and theoretical results relative to the Doppler effect are presented in table 5, as

TABLE 3

EFFECTIVE RESONANCE INTEGRAL MEASUREMENT: RESULTS AND COMPARISON WITH CALCULATION

Fuel identification	R_{ex}	σ_{ex} (%)	R_{th}
1	1.783	0.49	1.7828
2	2.455	0.69	2.4523
3	3.046	0.67	3.0292
4	3.250	0.42	3.2236

TABLE 4

ABSOLUTE VALUES OF THE MEASURED RESONANCE INTEGRALS

Fuel identification	RI (*b*)
1	$29.42 \pm 4.03\%$
2	$40.98 \pm 4.06\%$
3	$51.15 \pm 4.05\%$
4	$54.66 \pm 4.02\%$

TABLE 5

DOPPLER EFFECT MEASUREMENT: RESULTS AND COMPARISON WITH CALCULATION

Fuel identification	ϱ_{ex}	σ_{ex} (%)	ϱ_{th}	β_{ex} ($^oK^{-1}$)
1	1.197	0.65	1.196	$(1.05 \pm 0.04) \cdot 10^{-2}$
2	1.288	0.31	1.280	$(1.53 \pm 0.021) \cdot 10^{-2}$

ratios of the 1290 °K to the 293 °K values, with the 1/v capture subtracted (ϱ_{ex} and ϱ_{th}, resp.). In table 5 are also listed the corresponding experimental values of β_{ex} [$\beta_{ex} = (\varrho_{ex} - 1)/(\sqrt{T} - \sqrt{T_0})$] in the range from 293 °K to 1290 °K.

It can be noted that:

— The errors inferred from the dispersion of the experimental data agree with the corresponding error estimate carried out « a priori » by compounding the partial errors. This indicates the absence of significant systematic errors and that the error was in general correctly treated.

— The agreement between experimental and theoretical values is in general very satisfactory, i.e. almost within the limits of the quoted experimental error.

The last remark suggested to test the significance of a semi-empirical formula derived for β, extending the range of validity of the usual expressions [2] which cannot be generally applied to standard granulated fuel elements.

The formula was obtained starting from the expression of β for a single resonance [8]

$$\beta_n = \alpha_n F(T) \int_0^\infty \left\{ G(T,x) / [Y(T,x) + \alpha_n]^3 \right\} dx \quad (1)$$

where

β_n = Doppler coefficient for the n^{th} resonance;

α_n = σ_p / σ_{0_n};

σ_p = equivalent scattering cross section per absorbing atom;

σ_{0_n} = total « peak » cross section for the n^{th} resonance at 0 °K;

T = absolute temperature;

x = $(E - E_0) / \frac{\Gamma}{2}$ for the n^{th} resonance;

G, Y, F = appropriate functions.

Eq. (1) was derived for homogeneous media with resonance integrals sufficiently high to neglect interference scattering, but it can be applied to the usual heterogeneous systems on the basis of the equivalence theorems.

Deriving eq. (1) with respect to α_n

$$\frac{d\beta_n}{d\alpha_n} = \frac{\beta_n}{\alpha_n} - \alpha_n F(T) \int \frac{3\, G(T,x)\, dx}{[Y(T,x) + \alpha_n]^3 \cdot [Y(T,x) + \alpha_n]} \quad (2)$$

Calling b'_n an appropriate average value for $Y(T, x)$, eq. (2) becomes

$$\frac{d\beta_n}{d\alpha_n} = \frac{\beta_n}{\alpha_n} - \frac{3\,\beta_n}{b'_n + \alpha_n}, \quad (3)$$

whose general solution is

$$\beta_n = \left| a'_n\, \alpha_n / (b'_n + \alpha_n)^3 \right| + d' \quad (4)$$

From eq. (1) $\beta_n \to 0$ when $\alpha_n \to 0$; then $d' = 0$ and:

$$\beta_n = a'_n\, \alpha_n / (b'_n + \alpha_n)^3 = a_n\, \sigma_p / (b_n + \sigma_p)^3 \quad (5)$$

If RI_n is the contribution to the resonance integral by the n^{th} resonance,

$$\beta = \Sigma_n\, \beta_n\, RI_n / \Sigma_n\, RI_n = \Sigma_n\, \beta_n^* \quad (6)$$

with

$$\beta_n^* = RI_n\, \beta_n / \Sigma_n\, RI_n$$

The functions β_n^* show a similar behaviour (also quantitatively) for the low-energy resonances and exhibit their maxima at relatively high and close values of σ_p (about 1000 b), while for the less important resonances β_n^* is significant only if $\sigma_p < 100$ b. This consideration suggested the semi-empirical expression

$$\beta = A'\, \sigma_p + C' / (B' + \sigma_p)^3 \quad (7)$$

the term C' taking into account the contribution of the high-energy resonances.

For $RI < 100$ b, RI is proportional to $(\sigma_p)^{\frac{1}{2}}$ and eq. (7) may be written

$$\beta = A\, RI^2 + C / (B + RI^2)^3 \quad (8)$$

The measured resonance integrals at 293 °K (RI_0) for type 1 and type 3 fuels being 29.42 b and 51.15 b respectively, a best-fit of eq. (8) to ZUT-TUZ calculated values was performed in the range $20 \leq RI_0(b) \leq 60$, yielding

TABLE 6

COMPARISON OF THE VALUES OF THE DOPPLER COEFFICIENT β PREDICTED BY EQ. (9) WITH THE CORRESPONDING VALUES CALCULATED BY ZUT-TUZ AND EVALUATED BY EQ. (10)

	$10^2\,\beta$ ($^\circ K^{-\frac{1}{2}}$)		
RI_0 (b)	Eq. (9)	ZUT-TUZ	Eq. (10)
12.56	0.67	—	0.63 ± 0.03
20.34	0.80	0.81	—
22.96	0.85	—	0.83 ± 0.04
37.98	1.22	1.23	—
46.33	1.41	1.41	—
50.47	1.50	1.49	—
64.62	1.74	1.65	—
91.47	1.85	1.76	—
152.14	1.30	1.21	—

$$\beta = \frac{32.5\,x + 2.84}{(1.693 + x)^3} \cdot 10^{-2} \quad (^\circ K^{-1/2}) \qquad (9)$$

with

$$x = (RI_0/100)^2$$

The validity range of eq. (9) was verified to extend well outside the best-fit range, as shown in table 6 comparing the values of β predicted by eq. (9) with the corresponding β's calculated by the ZUT-TUZ codes over the range $20 \leq R\,I_0\,(b) \leq 150$, as well as with the β's evaluated by the empirical formula [2]:

$$\beta = 10^{-2}\left(0.58 + 0.5\,\frac{S}{M}\right)^\circ K^{-1/2}, \qquad 0.1 \leq \frac{S}{M} \leq 0.5\ cm^2/g \qquad (10)$$

at its limits of validity, i.e. $RI_0 = 12.56$ b, respectively 22.96 b.

The amplitude of the validity range of eq. (9) is taken as an index that the structure of the semi-empirical formula for β given by eq. (8) is substantially correct. A more careful best-fit procedure, as well as extending the best-fit range, would probably further improve the agreement already appearing from table 6. ■

Acknowledgments. The authors are indebted to the ECO reactor operation staff for technical assistance. The fuel particles were produced by AGIP Nucleare and coated by BELGONUCLEAIRE.

Received October 10, 1972

references

[1] G. CORBO: *Determinazione sperimentale dell'integrale di risonanza e dell'effetto Doppler in elementi combustibili a struttura granulare per reattori tipo HTR e confronto coi risultati di calcoli teorici.* Tesi di laurea. Politecnico di Torino (1971).
[2] E. HELLSTRAND, G. LUNDGREN: Nucl. Sci. and Eng., *12*, 435 (1962).
[3] A. BORUF, S. TASSAN: Nucl. Sci. and Eng., *25*, 365 (1966).
[4] W. W. ENGLE: K-1963 (1967).
[5] S. TASSAN, L. HAEMERS, A. BORUF: Energia Nucleare, 14, *5*, 289 (1967).
[6] L. W. NORDHEIM: GA 2527 (1961).
[7] G. F. KUNCIR: GA 2525 (1961).
[8] L. DRESNER: *Resonance absorption in nuclear reactors*, Pergamon Press (1960).

EUR 4861 e

COMMISSION OF THE EUROPEAN COMMUNITIES

PULSED SOURCE EXPERIMENTS WITH HEAVY WATER MODERATED NATURAL URANIUM LATTICES IN EXPO AND ECO

by

G. BIRKHOFF, L. BONDAR, W. HAGE and J. LEY

1972

Joint Nuclear Research Centre
Ispra Establishment - Italy

LEGAL NOTICE

This report is on sale at the addresses listed on cover page 4

at the price of B Fr 50 —

Commission of the
European Communities
D G XIII - C I D.
29, rue Aldringen
L u x e m b o u r g
October 1972

EUR 4861 e

COMMISSION OF THE EUROPEAN COMMUNITIES

PULSED SOURCE EXPERIMENTS WITH HEAVY WATER MODERATED NATURAL URANIUM LATTICES IN EXPO AND ECO

by

G. BIRKHOFF, L. BONDAR, W. HAGE and J. LEY

1972

Joint Nuclear Research Centre
Ispra Establishment - Italy

ABSTRACT

In 1967 several pulsed source experiments have been made at Ispra in the subcritical facility EXPO and the zero power critical reactor ECO. The aim of these experiments was to study the problems connected with pulsed source reactivity measurements in natural uranium, heavy water moderated reactors, which are mainly characterized by a long generation time as compared with the short living delayed neutron life time.

The paper contains a survey of various experimental and analytical methods applied along with the results of reactivity and generation time measurements in the negative reactivity range between about 0.17 and 40 $. The results are confronted with two group calculations, and systematic deviations are discussed. For the far subcritical cases a considerable deviation of about 5 % of the theoretical reactivity values remains unexplained.

This paper is a publication on an internal working document from January 1968.

KEYWORDS

ECO
SUBCRITICAL ASSEMBLIES
PULSED NEUTRON TECHNIQUES
REACTIVITY
MEASURED VALUES
ANALYTICAL. SOLUTION
COMPUTER CALCULATIONS

CONTENTS

EUR 4861 e

PULSED SOURCE EXPERIMENTS WITH HEAVY WATER MODERATED NATURAL URANIUM LATTICES IN EXPO AND ECO

by G. BIRKHOFF, L. BONDAR, W. HAGE and J. LEY

Commission of the European Communities
Joint Nuclear Research Centre - Ispra Establishment (Italy)
Luxembourg, October 1972 - 38 Pages - 7 Figures - B.Fr. 50.—

In 1967 several pulsed source experiments have been made at Ispra in the subcritical facility EXPO and the zero power critical reactor ECO. The aim of these experiments was to study the problems connected with pulsed source reactivity measurements in natural uranium, heavy water moderated reactors, which are mainly characterized by a long generation time as compared with the short living delayed neutron life time.

The paper contains a survey of various experimental and analytical methods applied along with the results of reactivity and generation time measurements in the negative reactivity range between about 0.17 and 40 $. The results are confronted with two group calculations, and systematic deviations are discussed. For the far subcritical cases a considerable deviation of about 5 % of the theoretical reactivity values remains unexplained.

This paper is a publication on an internal working document from January 1968.

1. DEFINITION OF THE PROBLEM

The time behaviour of the fundamental mode of the neutron density in a bare reactor after the injection of a neutron burst (δ - pulse) may be described by a sum of exponentials

$$n(t) = \sum_{i=o}^{m} A_i \; e^{-\alpha_i t} \tag{1}$$

$$\alpha_i = \frac{\beta+\rho}{\Lambda} + \frac{1}{\Lambda} \sum_{j=o}^{m} \frac{\beta_j \lambda_j}{\alpha_i-\lambda_j} = \alpha_p + \frac{1}{\Lambda} \sum_{j=o}^{m} \frac{\beta_j \lambda_j}{\alpha_i-\lambda_j} \tag{2}$$

$$A_i = \left(1 + \frac{1}{\Lambda\,(1+\rho)} \sum_{j=o}^{m} \frac{\beta_j \lambda_j}{(\alpha_i+\lambda_j)2}\right)^{-1} \tag{3}$$

This relation is obtained from the kinetic diffusion theory with the assumption of no retardation between the neutron populations of different energies, which is rather true for not too far subcriticality. The roots α_i of the socalled inhour equation (2) are all real and positive for the subcritical or delayed critical state ($\rho \geq o$). The numerically greatest root α_o is determined mainly by the prompt neutron decay constant α_p, while the remaining roots are closly related to the decay constants of the delayed neutron precursors.

In the case of a reactor of a long generation time, as we are dealing with, the contribution of the delayed neutrons to the decay constant α_o is negligible only for reactivities greater than about 7 $. It becomes however, significant near critical.

The variation of the neutron density with time, as described by (1) (2) (3) is true only for a fundamental mode neutron source distribution. In practice we are using a point source, which might be represented by a linear supperposition of the fundamental mode and an infinite number of harmonics.

The decay of the prompt neutron harmonics near critical is much faster than that of the fundamental mode. By a proper source-detector geometry it is possible to suppress certain important low order harmonics. After a certain waiting time only the fundamental mode of the prompt neutrons predominates. The situation becomes less favourable the more subcritical the reactor becomes.

In the case of a reflected reactor, as it is the ECO, the dynamic eigenfunctions differ from the static eigenfunctions. But the difference is rather small, as shown by FRAUDE (1), for a thin reflector like in ECO and might be neglected.

A special problem is the separation of the prompt neutrons from the delayed neutrons. The contribution of the delayed neutrons to the time variation of the neutron density is judged by the comparison of the amplitude and decay time ratios A_o/A_i and α_o/α_i respectively. For far subcriticality the ratios are great enough permitting to treat the delayed neutron contribution during the prompt decay as a constant. Near critical however, one must allow for the decay of the delayed neutrons during the prompt decay. The limit for the two situations can be set at the reactivity of about 5%.

In an actual pulsed source experiment it is necessary to repeat many times the pulsing of the reactor due to limitations in the source strength and the resolving time of the recording system. For a periodic pulsing at a repetition rate $R = 1/T$ with uniform δ bursts we get

$$n(t + N.T) = \sum_{i=o}^{m} A_i \, e^{-\alpha_i t} \cdot \left(\frac{1 - e^{-\alpha_i (N-1)T}}{1-e^{-\alpha_i T}}\right) \qquad (4)$$

The repetition rate is set as to allow for a complete decay of the prompt neutrons during one cycle.

With $T >> \frac{1}{\alpha_o}$ equation (4) may be written

$$n(t + N.T) = A_o e^{-\alpha_o t} + \sum_{i=1}^{m} A'_i e^{-\alpha_i t} \qquad (5)$$

with

$$A'_i = A_i \frac{1 - e^{-\alpha_i (N-1)T}}{1 - e^{-\alpha_i T}} \qquad (5a)$$

2. EXPERIMENTAL METHOD

A schematic of the pulsed source experiment is shown in Fig. 1, which represents a classical arrangement. As a pulsed neutron source the generator PHILIPS PW 5302/1 - with a maximum yield of about 3×10^{11} n/sec at a duty cycle of 3.10^{-4} was used. Starting the timer Ti, the multichannel scaler MCS (TMC, CN 110 A with plug in unit 212) stores in its first channel the background counts of the counting system. Next the neutron source generator is triggered. After a setable waiting time the registering of the counts per time intervall begins.
With the next trigger signal from the timer the cycle repeats and so on. The scaler SC serves for the counting of the inherent background. The following data recording procedure was generally followed.

1. Counting of the inherent background (neutron generator under high tension)
2. Start pulsing and recording
3. Stop pulsing after preset number of cycles but recording of the delayed neutron tail for about 15 min
4. Counting of the inherent background.

This data recording procedure delivers a counting rate distribution as described by equation (4) plus the higher harmonic contributions. It does not depend on the uniformity of the neutron bursts [2].

3. ANALYSIS METHODS

The analysis was generally restricted to the harmonic free part of the decay curve. Two types of analysis methods were applied. One is based on the determination of the prompt neutron decay constant (α_p-method)

the other on the evaluation of the prompt neutron and delayed neutron multiplication (integral method). The first method delivers

$$\frac{\rho}{\beta} = \alpha_p \frac{k\beta}{l} - 1$$

where $\frac{k\beta}{l}$ must be determined by a calibration meaurement with known reactivity, for instance at $\rho = 0$.
The second method gives $\frac{\rho}{\beta}$ directly.

3.1 α_p - Methods

3.1.1 Method I (SIMMONS, KING [3 7])

Conditioned by $\alpha_o >> \alpha_i \qquad i = 1, 2 \ldots m$

$A_o >> A_i$

$\alpha_o >> 1/T >> \alpha_i$

applied for $\approx \frac{\rho}{\beta} \geq 7\ \$$ with $\Lambda \approx 10^{-3}$ sec

The inhour equation is well approximated by

$$\alpha_o \approx \frac{\beta+\rho}{\Lambda} = \frac{1 - k\,(1-\beta)}{\Lambda \cdot k} = \alpha_p \qquad (6)$$

$$A_o \approx A_p \qquad (7)$$

$$\sum_{i=1}^{m} A_i' e^{-\alpha_i t} = \text{constant for } 0 \leq t \leq T \qquad (8)$$

$$n(t) = A_p e^{-\alpha_p t} + \text{const.} \qquad (9)$$

α_p is derived from a least squares fit of (9) on the harmonic free part of the experimental decay curve ($t \geq t_v$ = waiting time).

The check on the purity of prompt harmonics is made by varying the waiting time. In order to determine the reactivity in units of dollar a calibration meaurement for the evaluation of the reduced generation time $\frac{\Lambda}{\beta}$ is needed at known reactivity.

$$\frac{\rho}{\beta} = \alpha_p \cdot \frac{\Lambda}{\beta} - 1 \qquad (10)$$

3.1.2 Method II (FRAUDE [1])

Conditioned by $\alpha_o T >> 1$

applied for $\frac{\rho}{\beta} \leq 7\ \$$ with $\Lambda = 10^{-3}$ sec.

In this case the full expression for α_o must be taken

$$\alpha_o = \frac{\beta}{\Lambda}\left(1 + \frac{\rho}{\beta} + \frac{1}{\beta}\sum_{i=1}^{m}\frac{\beta_i - \lambda_i}{\alpha_o - \lambda_i}\right) = \alpha_p + \delta \qquad (11)$$

$$\frac{\rho}{\beta} = \alpha_o \frac{\Lambda}{\beta} - 1 + \frac{1}{\beta}\sum_{i=1}^{m}\frac{\beta_i - \lambda_i}{\alpha_o - \lambda_i} \qquad (12)$$

$\frac{\rho}{\beta}$ is found by the following iteration process.

From the meaurement we have

$$n(t) = C \cdot \left\{ A_o \cdot e^{-\alpha_o t} + \sum_{i=1}^{m} A_i e^{-\alpha_i t} \cdot \frac{1-e^{-\alpha_i (N-1)T}}{1-e^{-\alpha_i T}} \right\} \qquad (13)$$

$$n(T) = C \cdot \sum_{i=1}^{m} A_i e^{-\alpha_i T} \cdot \frac{1-e^{-\alpha_i (N-1)T}}{1-e^{-\alpha_i T}} \qquad (14)$$

With an initial guess of $\left(\frac{\rho}{\beta}\right)^{\circ}$ the roots of the inhour equation α_i and the A_i are calculated for $i = 1, 2, \ldots, m$. The normalisation factor C is obtained from (14).

A least square fit of $n_1(t) = C\,A_o\,e^{-\alpha_o t} = n(t) - C \sum_{i=1}^{m} \frac{A_i e^{-\alpha_i t}}{1-e^{-\alpha_i T}}$,

$t \geq t_w$ gives a first improvement of α_o.

With the α_o^o a new $(\frac{\rho}{\beta})^1$ is calculated by the equation (12).

The iteration goes on up to no improvement of α_o and $(\frac{\rho}{\beta})$ is achieved by further steps. Near critical the correction of α_o due to the delayed neutrons becomes important and the result is sensibly depending on the choice of the $\lambda_i \beta_i$ which are not well known mainly for the photo neutrons.
The values actually chosen are taken from Ref. [4_7] corrected by the best fitting efficiency coefficient for the photoneutron yield (see Table 1).
$\frac{\beta}{\Lambda}$ must be defined by a calibration meaurement at known criticality.

A check on the good choice of the β_i, λ_i is to compare the normalization factor

$$C = \frac{n(T)}{\sum_{i=1}^{m} \frac{A_i e^{-\alpha_i T}}{1-e^{-\alpha_i T}}} \qquad (15)$$

with the definition formula

$$C \cdot \sum_{i=o}^{m} A_i = C \quad \text{because} \quad \sum_{i=o}^{m} A_i = 1 \qquad (16)$$

taking the fitted $C.A_o$ value and the calculated C and A_i values ($i = 1, 2..m$)
This check permits also to estimate the contamination of the decay curve by prompt and delayed neutron harmonics.

3.2 Integral Methods

3.2.1 Method III (SJOSTRAND - GOZANI [5] [6])

Conditioned by $\alpha_o \gg \alpha_i \qquad i = 1, 2, \ldots, m$

$A_o \gg A_i$

$\alpha_o \gg 1/T \gg \alpha_i$

applied for $\approx \frac{\rho}{\beta} \geq 7\ \$$

The total multiplication factor of a fundamental mode neutron is proportional to

$$M_T = \frac{1}{1-k} \tag{17}$$

The prompt multiplication is proportional to

$$M_p = \frac{1}{1-k_p} = \frac{1}{1-k(1-\beta)} \tag{18}$$

From (17) and (18) it follows

$$\frac{M_p}{M_T - M_p} = \frac{1-k}{k\beta} \approx \frac{\rho}{\beta} \tag{19}$$

SJOSTRAND [5] has shown that for a reactor in the equilibrium state of the delayed neutrons, the integral over the fundamental mode prompt neutron density

$$n_{op}(t) = A_p . e^{-\alpha_p t}$$

extended over the period T is proportional to the prompt multiplication M_p. The integral over the total fundamental mode density

$$n_o(t) = \sum_{i=o}^{m} A_i e^{-\alpha_i t}$$

is proportional to the total multiplication factor M_T.

$$\frac{\int_o^T n_{op}(t)dt}{\int_o^T n_o(t)dt - \int_o^T n_{op}(t)\,dt} = \frac{M_p}{M_T - M_p} = \frac{\rho}{\beta} \qquad (20)$$

The separation of the prompt neutron density $n_{op}(t)$ from the total neutron density $n_o(t)$ is quite easy with the above condition $\alpha_o >> \alpha_i$ and $A_o \approx A_p$ because the total neutron density may be taken as a sum of the prompt neutron density and a constant part B forming the delayed neutron contribution. We get from (20)

$$\frac{\rho}{\beta} = \frac{A_p / \alpha_p}{B.T} \qquad (A_p\, e^{-\alpha_p T} \approx 0) \qquad (21)$$

Following the method of GOZANI [6] the fundamental mode distribution $n_{op}(t)$ is obtained from a least squares fit of the harmonic free part of the decay curve to

$$n_{op}(t) = A_p . e^{-\alpha_p t} \qquad (t \geq t_w) \qquad (22)$$

$$(n_{op}(t) = n_o(t) - B)$$

In this method it is assumed a fundamental mode distribution of the delayed neutrons. With a reasonable source detector geometry this is a rather good approximation because the delayed neutron density harmonics are much less excited than the prompt neutron harmonics. On the other hand they may play an important role if the source density distribution consists mainly of harmonics and the decay of harmonics is not much faster than the fundamental mode decay. With other words, if the total neutron density distribution during a pulsing period T is mainly consisting of higher harmonics. In such cases the results depend strongly on the source-detector geometry.

For a finite neutron burst duration (d) equation (19) must be replaced by

$$\frac{\rho}{\beta} = \left(\frac{A_p \, e^{-\alpha_p d} \cdot d}{1 - e^{-\alpha_p d}} \right) \cdot (B\,T)^{-1} \qquad (19a)$$

(normalization to a δ-pulse).

3.2.2 Method IV (BRONNER-DIO-SCHLOSSER [7])

Conditioned by $\alpha_o \gg 1/T$

$\approx \frac{\rho}{\beta} \leq 7\,\beta$

BRONNER et al. [7] have used a method which permits a simple separation of the prompt neutrons from the delayed neutrons even if the prompt decay is not much faster than the delayed neutron decay. The idea is to make a linear approximation of the exponential decay of the terms $A_i \, e^{-\alpha_i t}$, $i = 1, 2, \ldots, m$, $0 \leq t \leq T$

$$n_o(t) = A_o e^{-\alpha_o t} + \sum_{i=1}^{m} \frac{A_i e^{-\alpha_i t}}{1 - e^{-\alpha_i t}} \approx A_o e^{-\alpha_o t} + \sum_{i=1}^{m} \frac{A_i}{1 - e^{-\alpha_i t}} (1 - \alpha_i t) \qquad (23)$$

$$n_o(t) \approx A_o e^{-\alpha_o t} + B(o) + s.t = A_o e^{-\alpha_o t} + B(o) - \frac{B(o) - B(T)}{T} t \qquad (24)$$

The quantities A_o, α_o and B(o) are found by a least squares fit of the harmonic free total neutron density to (24). (B(T) is meaured).

$$\alpha_p = \frac{\Lambda + \rho}{\beta} = \alpha_o - \frac{1}{\Lambda} \cdot \sum_{i=1}^{m} \frac{\beta_i \lambda_i}{\alpha_o - \lambda_i} = \alpha_o - \delta \qquad (25)$$

Because the difference between B(o) and B(T) is due to the jump of the prompt neutrons at time 0, we have

$$A_p = A_o + (B(o) - B(T)) \qquad (26)$$

With (25) (24) (26) it follows from (20)

$$\frac{\rho}{\beta} = \frac{A_p}{\alpha_p} \cdot \left(\frac{A_o}{\alpha_o} + \frac{B(o) - B(T)}{2} T - \frac{A_p}{\alpha_p} \right)^{-1} \qquad (27)$$

In the case of a finite burst duration (d) equation (27) must be replaced by

$$\frac{\rho}{\beta} = \left(\frac{A_p e^{-\alpha_p d} \cdot d}{1 - e^{-\alpha_p d}} \right) \cdot \left(\frac{A_o e^{-\alpha_o d} \cdot d}{1 - e^{-\alpha_o d}} + \frac{B(o) - B(T)}{2} \cdot T - \frac{B(o) - B(T)}{2} d - \frac{A_p e^{-\alpha_p d}}{1 - e^{-\alpha_p d}} \right)^{-1} \qquad (28)$$

(normalization to a δ-burst)

3.2.3 Method V (GARELIS-RUSSEL- $\frac{k\beta}{\ell}$ method [8])

Conditioned by

$$\alpha_o \gg \alpha$$
$$\alpha_o \approx \alpha_p$$
$$A_o \approx A_p$$
$$\alpha_o \gg \frac{1}{T} \gg \frac{1}{\alpha_i}$$

applied for $\sim \frac{\rho}{\beta} \geq 7\ \$$

The socalled $\frac{k\beta}{\ell}$ method, introduced by GARELIS et al. [8] [2] is derived from the one group bare reactor kinetic equations where

$$S \equiv \frac{k_n \beta}{\ell_n} = \frac{k_\infty \beta}{\ell_\infty} = \frac{\beta}{\ell_c} \qquad (29)$$

One finds the following relation

$$\int_o^\infty n_p(t) e^{st}\, dt - \int_\partial^\infty n_p(t) dt = BT \qquad (30)$$

Equation (30) is valid also for the presence of prompt and delayed neutron harmonics.

The quantity $(\frac{k\beta}{\ell}) \equiv S$ is found by an iteration process of equation (30)

where $n_p(t)$ is the meaured total neutron density minus the constant delayed neutron density B.

In order to determine the reactivity $\frac{\rho}{\beta}$ the fundamental mode prompt neutron decay constant α_p must be determined too as described in 3.1 .

$$\frac{\rho}{\beta} = \frac{\alpha_p}{s} - 1 \tag{31}$$

4. DELAYED NEUTRON DATA

The effective fission delayed neutron yield β_i has been evaluated by taking into account the fast fission in U^{238} through the formula

$$\beta_i = \frac{\beta_i^8 \frac{\nu^8}{\nu^5} \delta_8 + \beta_i^5}{\frac{\nu^8}{\nu^5} \delta_8 + 1} \tag{32}$$

δ_8 was determined experimentally by Ref. [15]. Six fission delayed neutron groups are taken and the decay constants are those of the U^{235} fission neutrons. Efficiency coefficients of the photoneutrons stem from Ref. [16], but as pointed out in section 3.1.2 an empirical constant correction factor was applied for sake of best fitting the experimental decay curves near critical. Six photoneutron groups are regarded. A further correction due to the energy difference between prompt and delayed neutrons was applied.

$$\frac{k_p}{k_D} = e^{-B^2(\tau_p - \tau_D)}$$

5. THE COMPUTER PROGRAM

The analysis methods as described in section 3. (methods I, II, III, IV and V) have been coded in FORTRAN IV language for the data processing at the IBM 7090 machine. A block diagram of this computer program is given in Fig. 2.

6. EXPERIMENTAL SET-UP

6.1 EXPO Experiments

EXPO is a far subcritical bare reactor [10]. A schematic diagram of the EXPO facility is shown in Fig. 3. The facility was fueled with ECO reference elements (see Fig. 7). With the source location at the wall of the tank in the core midplane H/2 (H ⇒ D_2O level + extrapolation distances) only the odd numbered axial harmonics are excited as indicated in Fig. 4

$$\left(A_{n,o}\, e^{-\alpha_{o,n} t} \cos \frac{n\pi}{H} z \right)$$

The decay constants of the radial harmonics $A_{o,m}(t)$. $J_o(\nu_m \cdot r)$ with

$$A_{o,m}(t) = A_{o,m} e^{-\alpha_{o,m} t}$$

are a priori much higher compared with the axial harmonics due to the geometry of the tank (R << H). If we place the detector at

Z = H/3 we suppress the 3rd harmonic
Z = 2/5 H we suppress the 5th harmonic

putting the detector in the axis of the tank we suppress moreover all azimuthal harmonics.

The neutron detector utilized was a Li^6 glass scintillator with a photomultiplier of 19 mm ∅ (type 152 AVP) which was mounted on a rigid extension of 13 mm ∅ Al tube. It could be inserted into a Al guiding tube of 28 mm ∅ and 1 mm wall thickness running into the tank. All desired axial and radial positions of the detector could be realized. A fast tunnel diode discriminator [+)] was fed directly with the PMP pulses. The dead time of the total counting equipment is about 10^{-7} sec permitting a peak counting rate of about 5.10^5 c/sec without significant dead time correction. By this way it was possible to operate the pulsed source at its maximum yield and to achieve a high signal to inherent background ratio which is important for the accuracy of the integral methods (III, IV, V).

+) The electronic equipment was designed and constructed by the Electronics Service.

6.2 ECO Experiments

The critical facility ECO is described in Ref. [11]. A schematic view is shown in Fig. 5. The only accessible positioning of the pulsed source was a horizontal channel in the bottom reflector as indicated in the Fig. 5 . This position of the pulsed source is very unfavourable from the harmonics excitation point of view. It is of course possible to arrange for a better source position with certain modification on the pulsed source or reactor. But is was found rather inconvenient for the purpose of the experiments which was limited to the study of the method itself.
The detector used was partly a Li^6 glass scintillator as described in 5.1 or a BF_3 proportional counter (28EB40 of 20th Century) depending on the neutron peak flux at the detector position.

7. RESULTS

7.1 EXPO Measurements

Two types of lattices were investigated in the EXPO facility.

- U-19-12/OMPH coolant fuel elements
- U/19-12/Diphyl coolant fuel elements.

With the U-19-12/OMPH fuel elements a series of measurements was made with a lattice of 26.6 cm square pitch completely filling the tank cross section (bare system).
Regarding the assumptions of the GARELIS (V) and the SJOSTRAND (III) methods these are quite well fulfilled in that case. In particular have been checked the dependence of the results on the detector position and the duration of the neutron burst for two different core heights H of 260 cm and 230 cm.

In Table 2 the results of these measurements are summarized and compared with homogeneous two group calculations [12].

In Table 3 are given the results of the meaurements with the U-19-12/diphyl fuel elements. The meaurements have been done with two full core loadings of square lattices with 18.0 cm and 26.6 cm.

The theoretical ($\frac{\rho}{\beta}$) values are derived from the two group formula:

$$\frac{\rho}{\beta} = \frac{(1+L^2B^2)(1+\tau B^2) - k_\infty}{\beta\, k_\infty} \qquad (33)$$

From the formula

$$S = \frac{k\,\beta}{\ell} = \frac{k_\infty \beta}{\ell_0(1+\tau B^2)} = \frac{\beta}{\Lambda} \qquad (34)$$

the generation time has been computed. L^2, τ, k_∞ and ℓ_0 are calculated by the lattice code PINOCCHIO [12].
The given error limits are due to the estimated error of β ($\frac{\Delta\beta}{\beta} = \pm 5\ \%$) and the uncertainty of the geometrical buckling $\Delta B^2_{\rho o} = \pm 0.1\ m^{-2}$.

The quoted error limits of the experimental results represent the linear term of the Taylor series of the ($\frac{\rho}{\beta}$)-perturbed formulae (21) and (31).

$$\Delta\left(\frac{\rho}{\beta}\right)_{III} = \frac{1}{\alpha_p BT}\left(\Delta A_p + \frac{A_p}{\alpha_p}\Delta\alpha_p + \frac{A_p}{B}\Delta B\right) \qquad (35)$$

$$\Delta\left(\frac{\rho}{\beta}\right)_V = \frac{1}{S}\left(\Delta\alpha_p + \frac{\alpha_p}{S}\Delta S\right) \qquad (36)$$

$$S \equiv \frac{k\beta}{\ell}$$

ΔA_p and $\Delta\alpha_p$ are estimated from results of exponential fits on experimental curves with different waiting times t_w.
ΔB is the standard deviation of the measured delayed neutron density. The value of ΔS is obtained by evaluating the quantity $S = \frac{k\beta}{\ell}$ with the delayed neutron density varied within the error limits $\pm\Delta B$. From the results we conclude:

a) there is no clear influence on the results by the pulse duration between 7 µsec and 50 µsec.
b) the results of the GOZANI method (III) are more sensitive to the harmonics than the CARELIS method (V). Positive harmonics tend to reduce the reactivity value obtained from method III, while negative harmonics do the contrary. No clear effect was observed for the CARELIS method (V).

c) in the most favoured counter position which delivers the smallest harmonics effect, the results of both methods agree within their error limits but method III gives systematically little bit higher values.

d) the meaured reactivity values deviate by about 15 % from the calculated values using homogeneous two group theory with PINOCCHIO core parameters. This discrepancy, which appears for the ECO experiments too, is discussed below in section 7.3

7.2 ECO Measurements

Determination of prompt neutron decay constant at delayed critical

The prompt neutron decay constant at delayed critical $\alpha_{pc} = \frac{\beta}{\Lambda_c}$ was determined from the meaurement of α_o as a function of the D_2O level H with $H < H_{crit.}$ α_p is obtained from eq. (25). As the correction term

$$\frac{1}{\Lambda} \sum_{i=1}^{m} \frac{\beta_i \lambda_i}{\alpha_o - \lambda_i}$$

is rather small even near critical the precision of the λ, β_i, λ_i need not to be very high. Λ is defined with sufficient accuracy by the integral method (IV) (see 3.2).

In the one group approximation α_p is a linear function of $(\frac{1}{H^2})$ while in the two group theory higher order terms of $(\frac{1}{H^2})^n$ appear. In all experimental cases, however, the higher order terms are negligible.

The effective core height $H = H' + \Delta H$,

$H' \Rightarrow$ measured D_2O level

$\Delta H \Rightarrow$ correction due to the calibration of the D_2O level meter, the linear extrapolation distances and the bottom reflector saving was evaluated from the relation

$$\frac{1}{(H'_{crit} + \Delta H)^2} = \frac{\gamma^2}{\pi^2} = \frac{1}{H^2_{crit.}} \qquad (36)$$

where γ^2 is the axial buckling meaured in a flux mapping experiment [13].

In Fig. 6 the prompt decay constant is plotted against $\frac{1}{H^2}$ from which α_{pc} is obtained. The reactivity values for different D_2O level are derived from the "two group corrected" formula.

$$\frac{\rho}{\beta} = \frac{\alpha_p}{\alpha'_{pc}} - 1 \qquad (37)$$

$$\alpha'_{pc} = \alpha_{pc} \cdot \frac{1+\tau B_c^2}{1+\tau B_{go}^2} = \frac{\beta}{\Lambda} \qquad (38)$$

with $$B_{go}^2 = \frac{\pi^2}{H^2} + \mu^2 \quad , \quad B_c^2 = \frac{\pi^2}{H_{crit}^2} + \mu^2$$

μ^2 is the experimentally determined radial buckling [13].

The reactivity values obtained for different D_2O levels are listed down in Table 4. The quoted error limits are derived in the same way as described under section 7.1 . As pointed out above the accuracy of these measurements were hindered by the unfavourable source and detector positions. Nevertheless the methods I and II should in principle deliver meaningful results. On the other hand the integral methods failed completely at $\frac{\rho}{\beta} > 3\ \$$ due to the strong excitation of higher harmonics. Near critical the inherent neutron background was very high as compared with the neutron density originating from the pulsed source (low signal to noise ratio) effecting in a negative sense the measurement of the delayed neutron density. The results of the integral methods are therefore meaningless, but they demonstrate the dependency of these methods on the source-detector geometry.

7.2.2 Reactivity of Safety Rods

The reactivity value of the two safety rods of ECO have been measured. After the reactor was balanced to criticality one of the safety rods or both together were droped into the reactor. After the decay of the short living delayed neutron precursors the pulsed source was started.
Table 5 shows the results of the different meaurements.
For comparison the reactivity values obtained by the rod drop method [13] are included. The variation of the neutron generation time due to the safety rod has been neglected, because this effect should be rather small.

The agreement with the results of the method II is not very satisfactory but just at the error limits. In order to clearify the discrepancy the accuracy of the pulsed source must be improved by a proper source detector arrangement.

7.3 The Neutron Generation Time

The reduced neutron generation time $\frac{\Lambda_c}{\beta} = \frac{1}{\alpha_{pc}}$ at delayed critical was compared with the calculated one using homogeneous core parameters from the PINOCCHIO [12]. Actually the neutron generation time was calculated by the following two group formula for a reflected reactor (see [1]).

$$\Lambda_c = \frac{\frac{1}{v_1}\int_V \phi_1^+ \phi_1 \, dV + \frac{1}{v_2}\int_V \phi_2^+ \phi_2 \, dV}{\frac{k_\infty \Sigma_a}{p}\int_V \phi_1^+ \phi_2 \, dV} \qquad (39)$$

The flux times adjoint flux integrals were computed by the code EQUIPOISE 3 [14].

A comparison between the measured and the calculated generation time was made too for the cases of EXPO for subcritical experiments. The calculated values are computed by the bare reactor two group formula using PINOCCHIO homogeneous core parameters.

$$\frac{\Lambda}{\beta} = \frac{\ell_c}{\beta} \cdot \frac{1 + \tau B_g^2}{1 + \tau B_c^2} \qquad (40)$$

Table 6 shows the results.

The quoted error of the calculated reduced generation time takes into account an uncertainty of the effective delayed neutron fraction β and of the geometrical and critical buckling formula (40). For the experimental results the error propagation of the formulas

$$\frac{\Lambda}{\beta} = \frac{1}{\alpha_p}\left(\frac{\rho}{\beta} + 1\right) \qquad (41)$$

or

$$\frac{\Lambda}{\beta} = \frac{1}{\frac{k\beta}{\ell}} = \frac{1}{\beta} \qquad (42)$$

was computed taking the uncertainty of the experimental quantities α_p, $\frac{\rho}{\beta}$ and S respectively.

For the ECO experiment the calculated reduced generation time differs by about 16 %. Regarding the error limits in the optimistic case a deviation of + 3 % remains. It is thought that the difference is due to an overestimation of the calculated thermal neutron life time.

The tendency of the deviation between calculated reduced generation time becomes stronger for the cases of all EXPO experiments. This tendency may be explained partly by the influence of the leakage correction term of equation (40) which is incorrect at least due to the known underestimation of B_c^2 in PINOCCHIO by about 15 %. Apart from this the discrepancy would suggest an increase of β by at least 5 % which is certainly unreasonable. Therefore it is thought on a systematic error of the measured reduced generation time of about - 5 %. As a consequence the reactivity of the EXPO measurements evaluated by the GOZANI and GARELIS methods are both underestimated by about 5 % No reason for this systematic error has been found, however.

8. CONCLUSIONS

Reactivity measurements in far subcritical bare heavy water assemblies are possible with a relative precision of about $\pm$ 3 %. The neutron generation time seems,however, overestimated by about 5 % corresponding to an underestimation of the absolute reactivity value by 5 %. A heterogeneous kinetic eigenvalue calculation of the investigated strong heterogeneous lattices will be executed next, in order to study this discrepancy. A static heterogeneous code (3-group monopoles and dipoles) will be adapted to this calculus. Near critical, reactivity measurements are possible with good accuracy in the relative and absolute value provided the source-detector geometry is reasonable. Uncertainties in β_{eff} do not enter into the directly measured reactivity in dollar units ($\rho^* = \rho/\beta_{eff}$).

ACKNOWLEDGEMENTS

The authors are indebted to the Electronics Service for the very good functioning of their electronic equipment utilized in the experiments especially to Mr. G.COLOMBO, A. PEDRINI, L. STANCHI. Thanks are given to the ECO operational group for their collaboration during the ECO experiments.

SYMBOLS USED

α_p	Prompt neutron decay constant
α_i	Decay constant
A_i	Amplitude
β_i	Delayed neutron fraction of group i
λ_i	Delayed neutron precursors decay constant of group i
β	Effective delayed neutron fraction
k	Effective multiplication constant
ℓ	Effective thermal neutron life time
Λ	Generation time
p	Resonance escape probability
ρ	Negative reactivity $\rho = \frac{1 - k}{k}$
B	Equilibrium state delayed neutron density
T	Pulsing period
A_p	Prompt neutron amplitude
t_w	Waiting time
d	Duration of neutron burst
k_n	Eff. multiplication of the n^{th} mode
ℓ_n	Eff. life time of the n^{th} mode neutron
k_∞	Infinite medium multiplication factor
ℓ_∞	Infinite medium neutron life time
α_{pc}	Prompt neutron decay constant at delayed critical
ℓ_c	Prompt neutron life time at delayed critical
$B^2_{g_n}$	Geometrical buckling of the n^{th} mode
B^2_c	Critical buckling
L^2	Thermal neutron diffusion area
τ	Slowing down area
$\phi_{1/2}$	Fast/slow neutron flux
$\phi^\ddagger_{1/2}$	Fast/slow neutron adjoint flux
δ_8	Fast fission ratio
ν^5/ν^8	U^{235}/U^{238} neutron yield per fission
v_1/v_2	Fast/slow neutron velocity
S	$\equiv \frac{k\beta}{\ell}$

Group	λ_i [sec^{-1}]	β_i	remark
1	3.87	$2.54.10^{-4}$	F
2	1.40	$1.07.10^{-3}$	F
3	$3.11.10^{-1}$	$3. 0.10^{-3}$	F
4	$2.77.10^{-1}$	$2.34.10^{-4}$	P
5	$1.15.10^{-1}$	$1.36.10^{-3}$	F
6	$3.17.10^{-2}$	$1.48.10^{-3}$	F
7	$1.69.10^{-2}$	$7.33.10^{-5}$	P
8	$1.27.10^{-2}$	$2.52.10^{-9}$	F
9	$4.81.10^{-3}$	$2.48.10^{-5}$	P
10	$1.50.10^{-3}$	$1.19.10^{-3}$	P
11	$4.28.10^{-4}$	$7.43.10^{-6}$	P
12	$1.17.10^{-4}$	$8.42.10^{-6}$	P
		$\beta=7.77.10^{-3}$	

TABLE 1: Delayed neutron data (without fast leakage correction $e^{-B_i^2(\tau_p-\tau_d)}$)

F $\Longrightarrow$ fission neutrons

P $\Longrightarrow$ photoneutrons

N°	Core height	burst duration	(see fig. 4) detector pos. Z	Method I	kβ/ℓ	Method V	PINOCCHIO	
	H(cm)	(/usec)	(cm)	ρ/β (%)	(sec^{-1})	ρ/β (%)	kβ/ℓ	ρ/β
1	230.	7.	1	36.4 ±1.3	7.35 ±.08	35.4 ± .7	5.96 ±.30	42.3 ±2.6
2	230.	50.	1	36.6 ±1.0	7.23 ±.08	35.8 ± .6		
3	230.	7.	3	38.4 ±1.8	7.07 ±.08	37.5 ± .7		
4	230.	50.	3	37.1 ±1.2	7.24 ±.08	36.3 ± .7		
5	260.	7.	3	36.3 ±0.9	7.05 .08	35.1 ± .7	6.05 ±.31	40.4 ±2.5
6	260.	50.	3	35.4 ±0.8	7.17 ±.08	34.4 ± .6		

TABLE 2: Results of pulsed source reactivity measurements in EXPO with U 19 12 OMPH fuel elements

TABLE 2: (follows)

N°	Core height	burst duration	(see fig. 4) detector pos. Z	Method I	kβ/ℓ	Method V	PINOCCHIO	
	H(cm)	(μsec)	(cm)	ρ/β ($)	(sec^{-1})	ρ/β ($)	kβ/ℓ	ρ/β
7	260.	7.	2	35.7 ±1.1	7.34 ±.08	33.5 ± .8		
8	260.	50.	2	37.5 ±1.1	6.90 ±.08	35.4 ± .7		
9	260.	7.	5	38.6 ±1.5	7.66 ±.08	31.7 ± .7		
10	260.	50.	5	42.4 ±1.8	6.88 .08	35.3 ±1.0		
11	260.	7.	1	33.8 ±1.3	7.20 0.08	34.4 .7		
12	260.	50.	1	33.8 ±1.0	7.19 .08	34.5 .7		
13	260.	7.	4	39.6 ±2.3	7.07 .08	34.2 ±1.2		

						METHOD III	METHOD V		PINOCCHIO	
pitch (cm)	el.N°	A_p (counts/ sec)	α_p (sec^{-1})	B (counts/ sec)	T (sec)	$\frac{\rho}{\beta} = (\frac{A_p}{\alpha_p})(B.T)^{-1}$ in $	β/Λ (sec^{-1})	ρ/β ($)	β/Λ sec	ρ/β ($)
23.0	32	$9.35.10^{-4}$ ± 15	253 ±2	309 ±3	0.05	23.8 ±.8	10.87 ±.12	22.2 ±.4	9.04 ±.5	25.2 ±1.4
26.6	24	$1.42.10^{5}$ ±.01	245 ±2	356 ±3	0.05	32.0 ±.9	7.79 ±.09	30.3 ±.6	6.24 ±.4	36.0 ±1.9

TABLE 3: Results of pulsed source reactivity measurements in EXPO with U-19-12/Diphyl fuel elements

U-19-12 Diphyl coolant
D_2O title / 99.72%
T = 22 ± 2°C

$\beta = \beta_{eff}$ = 00079 ± 5%

D_2O level (cm)	α_p (sec^{-1})			ρ/β ($)					remark see fig. 5
	Method I	II	IV	I	II	III	IV	V	
110.14	77.2±1			6.55±0.65		18.4		21.1	counter pos.1
116.14	66.0±2			6.48±0.55		12.8		15.3	1
114.57	30.8±1	32.7±1	32.2±1	(2.06)	2.24±0.27	(3.51)	3.54	(4.6)	2
153.55	18.4	20.5±1	20.1±1	(0.83)	1.04±0.2	(1.51)	1.55	(2.05)	2
160.0	13.0	15.7±1	14.1±1	(0.30)	0.56±0.18	(0.75)	0.78	(1.65)	2
164.55	–	11.7±1	10.6±1	–	0.17±0.16	–	0.28	–	
167.6	extra-polated	10.0±0.5			0.0				

TABLE 4: Results of pulsed source reactivity measurement in ECO with U-19-12 diphyl fuel elements at different D_2O water level

D_2O title: 99.69

Core loading: pitch 23.5 cm, 119 fuel elements

rods inserted	α_p (sec^{-1})		ρ/β ($)			remarks see fig. 5
	Method II	IV	II	IV	rod drop	
1	23.6±1	22.7±1	1.34±0.21	1.95	1.65±0.17	counter pos. 2
2	32.7±1	32.0±1	2.24±0.27	3.61	2.87±0.23	" " 2
2	33.9±1	33.0±1	2.36±0.27	3.73		" " 1

TABLE 5: Reactivity of ECO safety rods

core loading: pitch 23.5 cm, 119 fuel elements

D_2O title: 99.69

$\beta = \beta_{eff} = 0.777 \pm 5\%$

Lattice pitch (cm)	fuel type	Λ/β [sec]		Remark
		Experim.	Theory	
23.5	U-19-12-diphyl	0.100 ±.005	0.116 ±.008	Method II, ECO critical
23.0	" "	0.0980 ±.0012	0.110 ±.005	Method I, EXPO
23.0	" "	0.0919 ±.0009		Method V, EXPO
26.6	" "	0.131 ±0.002	0.160 ±.009	Method I, EXPO
26.6	" "	0.128 ±.001		Method V, EXPO
26.6	" OMPH	0.146 ±.002	0.167 ±0.009	Method I, EXPO
26.6	" "	0.141 ±.002		Method V, EXPO

TABLE 6: Reduced generation time derived from ECO and EXPO measurements

REFERENCES

[1] A. FRAUDE
Nukleonik, 4 (1962) 84

[2] E. GARELIS
Nucl. Sci.Eng. 18 (1964) 242

[3] B.E. SIMMONS, J.S. KING
Nucl. Sci. Eng., 3 (1958) 895

[4] KEEPIN, G.R.
Nucleionics 20, 8 (1962) 150

[5] N.G. SJOSTRAND
Arkiv for Fysik 11 (1957) 233

[6] T. GOZANI
Nukleonik 4 (1962) 348

[7] G. BRONNER et al.
Sympos. on pulsed neutron research
Karlsruhe, May 10-14, 1965, paper SM 6216

[8] E. GARELIS, J.L. RUSSEL
Nucl. Sci. Eng. 16 (1963) 263

[10] Research at Ispra 1961-1967
EUR 3940.e -1 , p. 42 - 47

[11] G. BLAESSER et al.
EUR 130.f (1962)

[12] L. AMYOT et al.
EUR 4231.e (1969)

[13] W. HAGE et al.
ATKE 13 - 26 (133 - 138) 1968

[14] T.B. FOWLER, M.C. TOBIAS
EQUIPOISE 3, ORNL 3199

[15] G. MARACCI and F. RUSTICHELLI
Journal of Nuclear Energy, 1967 (Vol.2)

[16] U. CANALI et al.
EUR 205.f (1963)

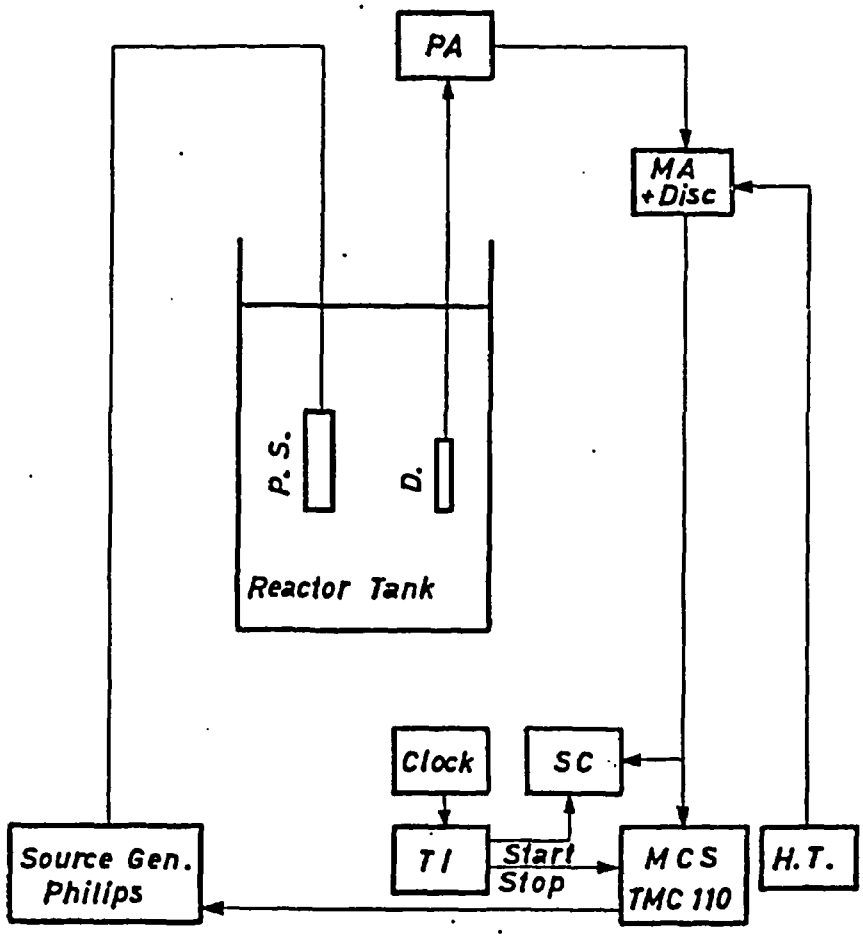

Fig.1 Block diagram: pulsed source experiment

D	Detector
PA	Preamplifier
MA+Disc	Main amplifier and discriminator
HT	High tension unit
MCS	Multichannel scaler
TI	Timer
PS	Pulsed source

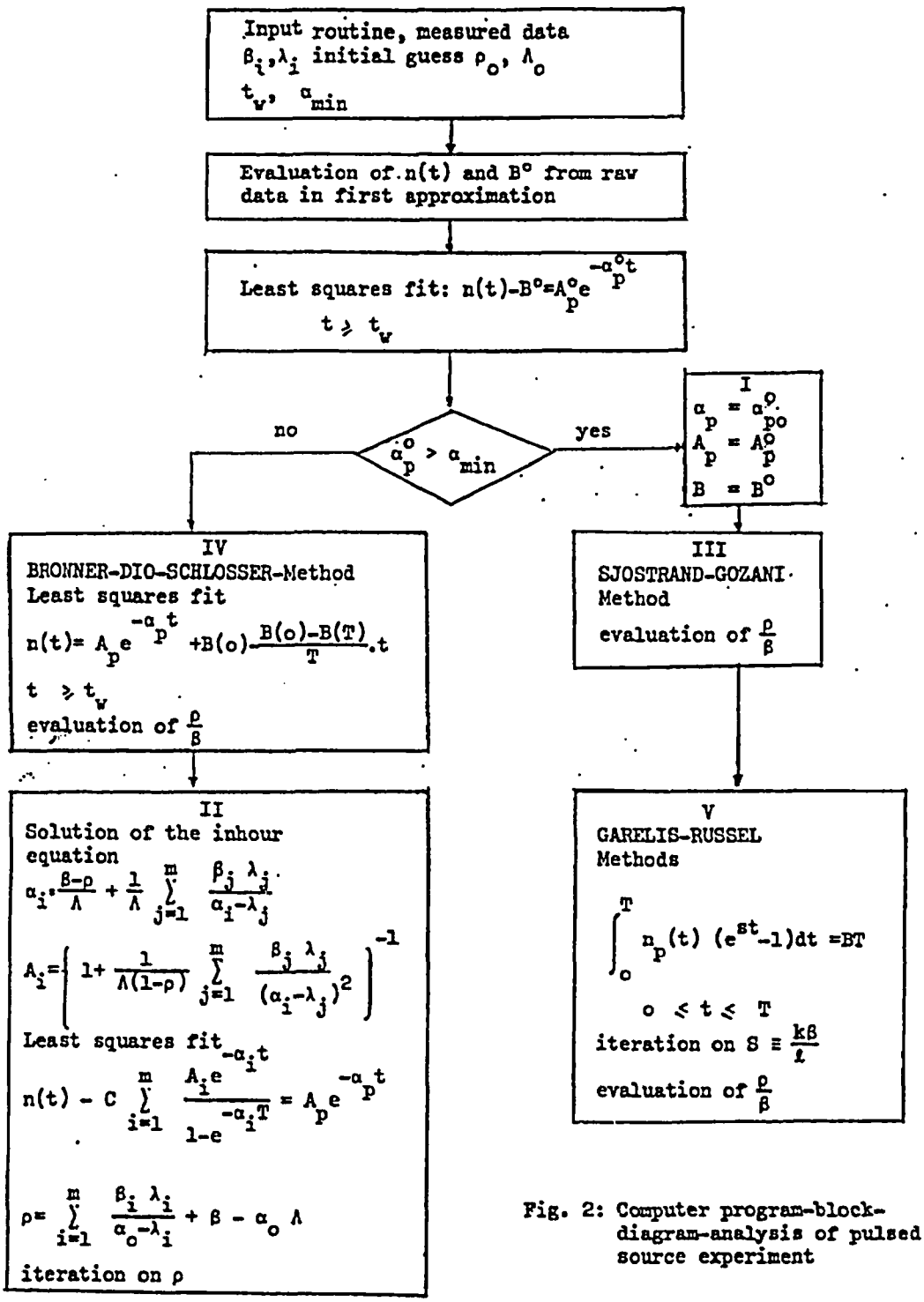

Fig. 2: Computer program-block-diagram-analysis of pulsed source experiment

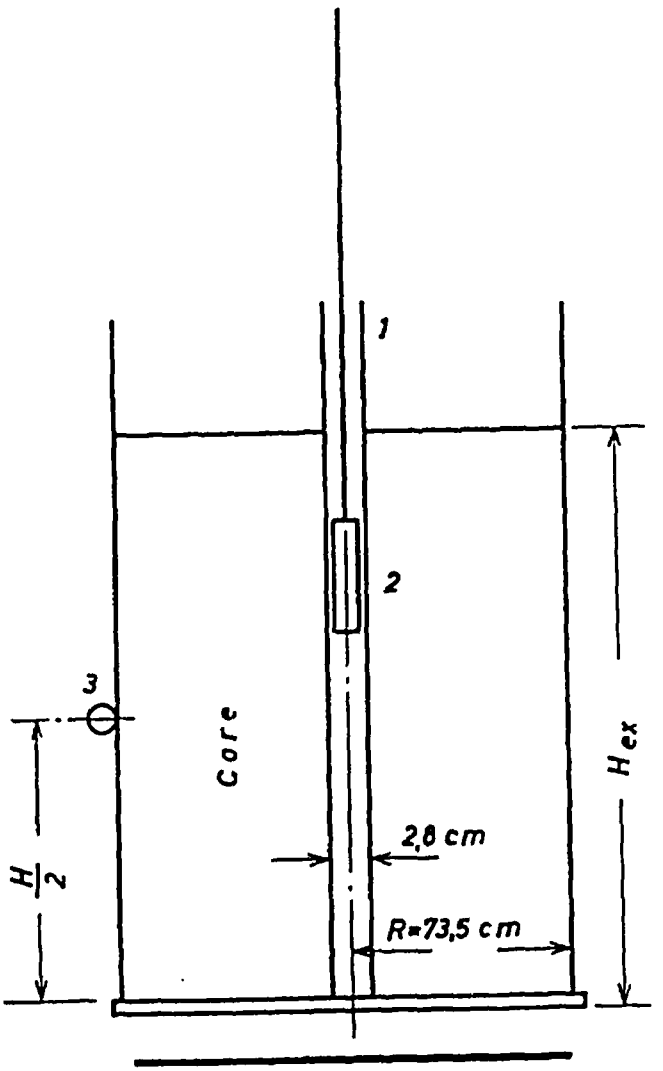

1. Guiding tube of Al
2. Detector
3. Pulsed source

Fig.3 - Geometrical arrangement for pulsed-source experiments on Expo.

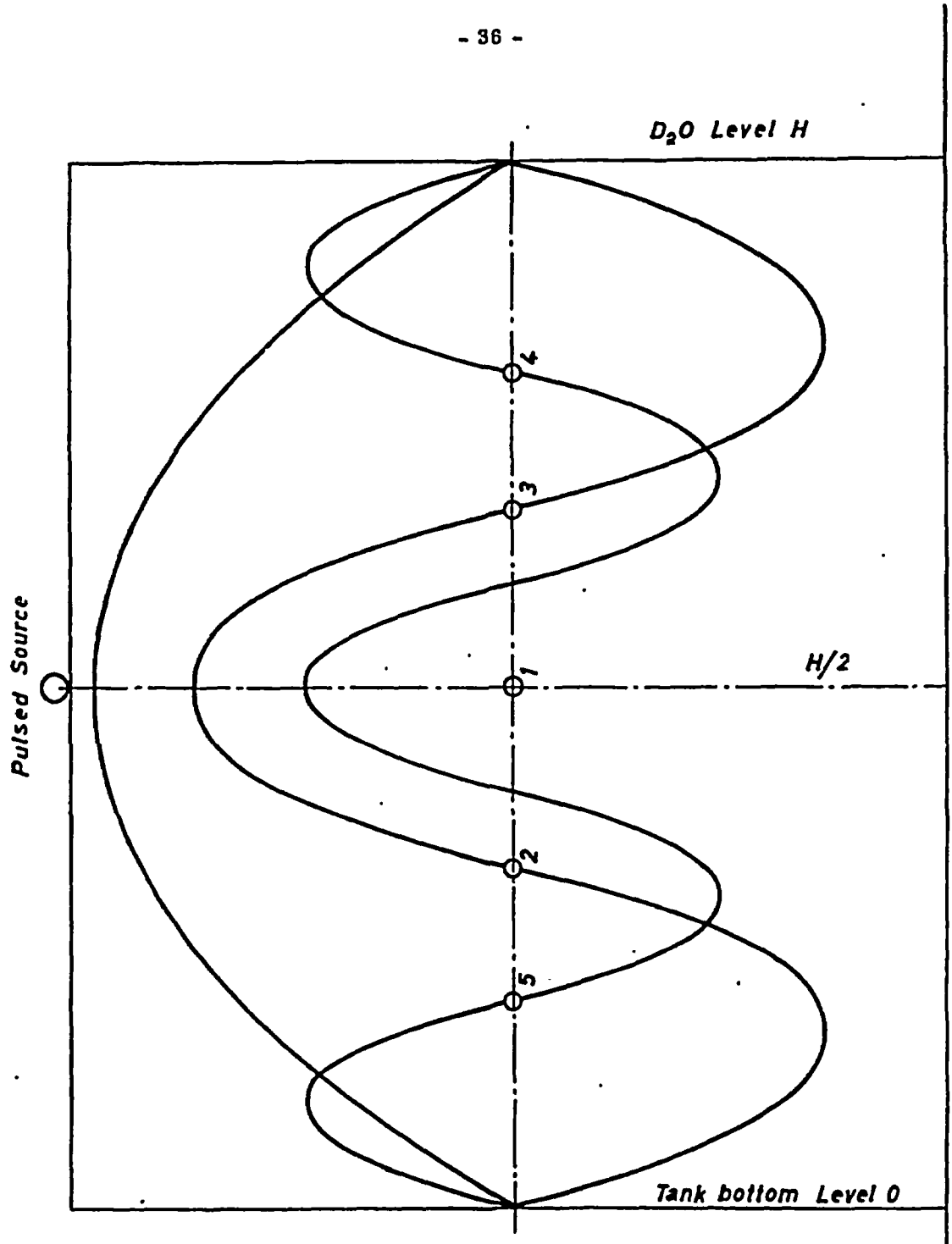

Fig.4 - Excitation of axial harmonics due to source arrangement at core midplane

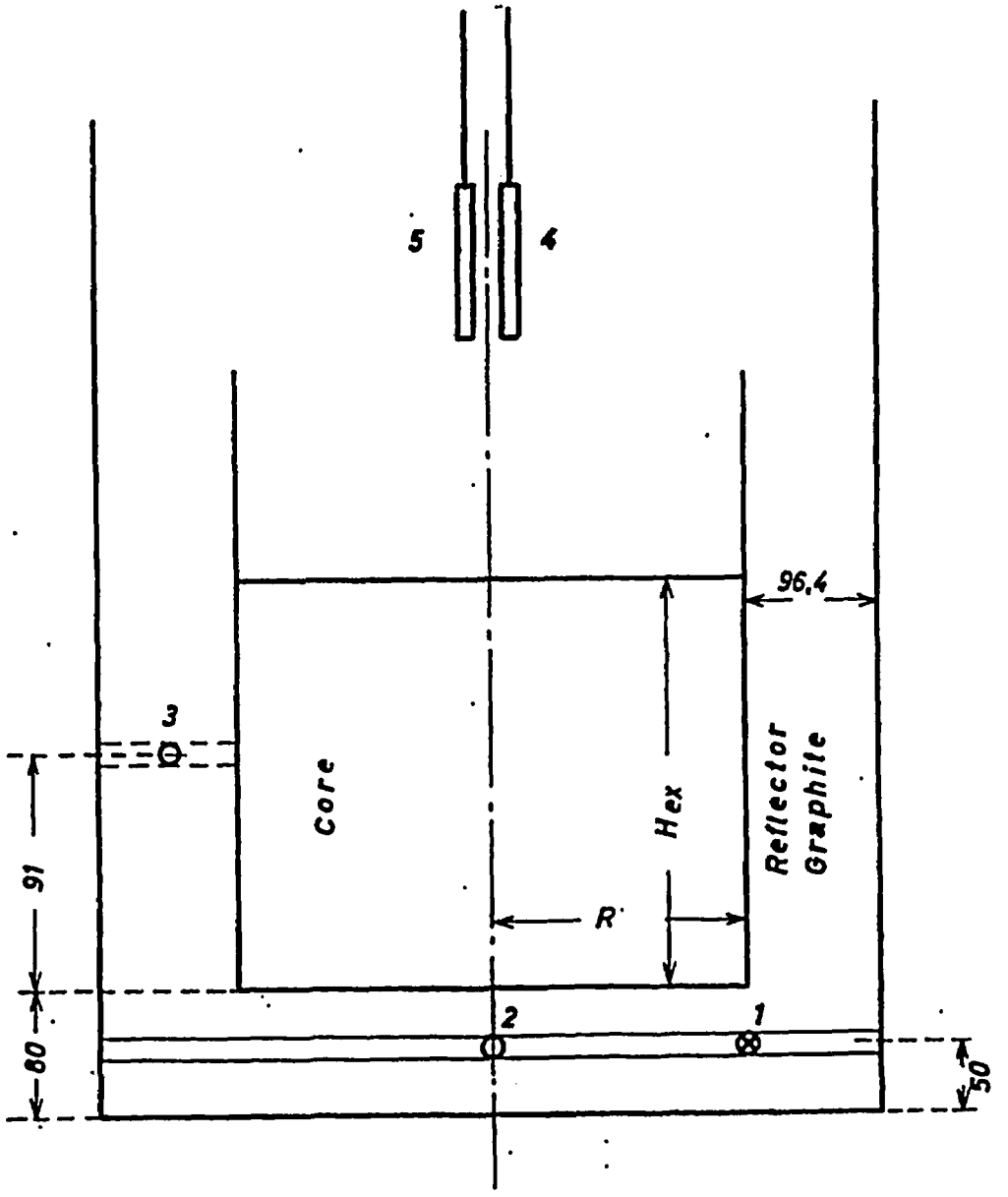

Fig. 5 - Geometrical arrangement of pulsed source measurements on ECO

1. Pulsed source
2. Detector, Pos.1
3. Detector, Pos.2 (Azimutally displaced by 90°)
4. Safety rod 1
5. Safety rod 2

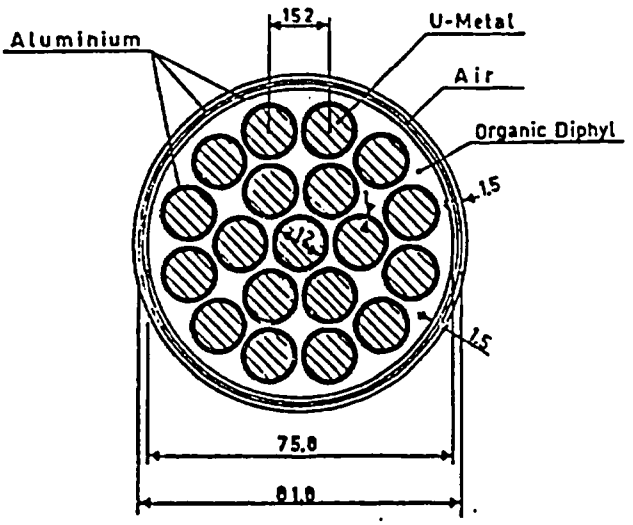

Fig. 7 - "ORGEL"-type fuel element: cluster of 19 uranium metal rods (UM-19).

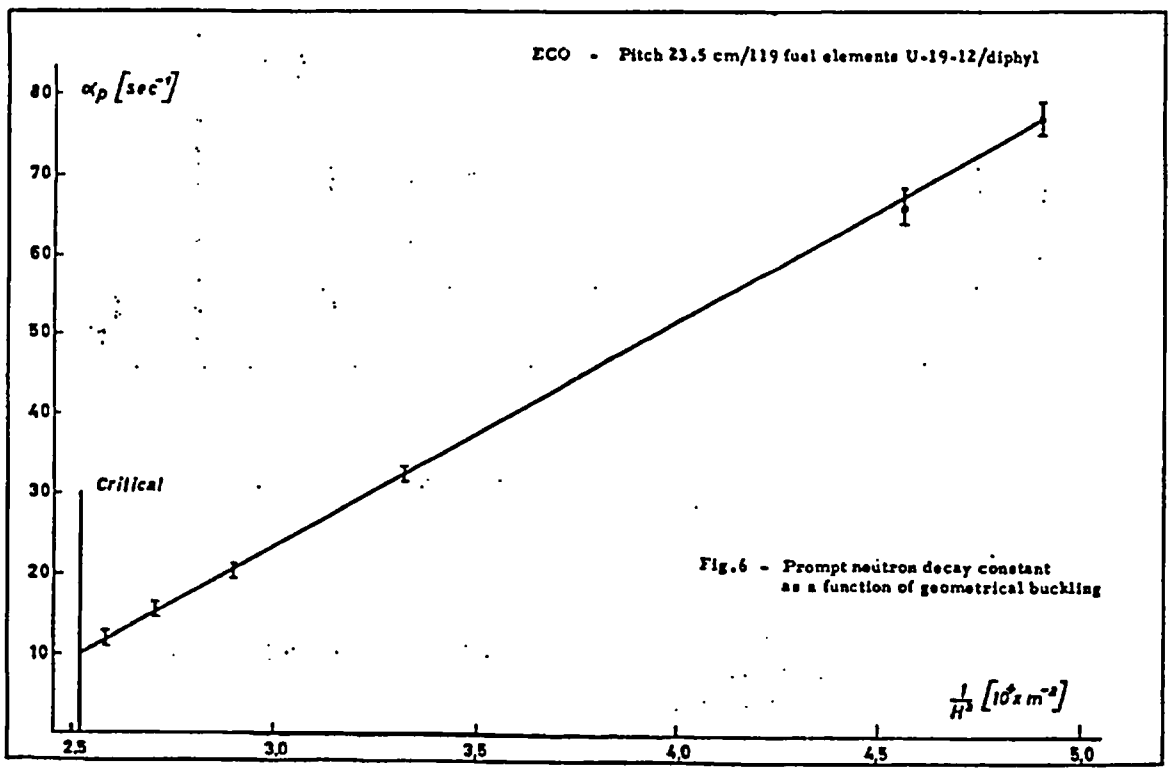

Fig.6 - Prompt neutron decay constant as a function of geometrical buckling

To disseminate knowledge is to disseminate prosperity — I mean general prosperity and not individual riches — and with prosperity disappears the greater part of the evil which is our heritage from darker times.

Alfred Nobel

SALES OFFICES

The Office for Official Publications sells all documents published by the Commission of the European Communities at the addresses listed below, at the price given on cover. When ordering, specify clearly the exact reference and the title of the document.

GREAT BRITAIN AND THE COMMONWEALTH

H M Stationery Office
P O Box 569
London S E 1

UNITED STATES OF AMERICA

European Community Information Service
2100 M Street, N W
Suite 707
Washington D C 20 037

BELGIUM

Moniteur belge — Belgisch Staatsblad
Rue de Louvain 40 42 — Leuvenseweg 40 42
1000 Bruxelles — 1000 Brussel — Tel 12 00 26
CCP 50 80 — Postgiro 50 80

Agency
Librairie européenne — Europese Boekhandel
Rue de la Loi 244 — Wetstraat 244
1040 Bruxelles — 1040 Brussel

GRAND DUCHY OF LUXEMBOURG

Office for official publications of the European Communities
Case postale 1003 — Luxembourg 1
and 29 rue Aldringen Library
Tel 4 79 41 — CCP 191 90
Compte courant bancaire BIL 8 109/6003/200

FRANCE

Service de vente en France des publications des Communautés européennes
26, rue Desaix
75 Paris-15e — Tel (1) 306 5100
CCP Paris 23 96

GERMANY (FR)

Verlag Bundesanzeiger
5 Koln 1 — Postfach 108 006
Tel (0221) 21 03 48
Telex Anzeiger Bonn 08 882 595
Postscheckkonto 834 00 Koln

ITALY

Libreria dello Stato
Piazza G Verdi 10
00198 Roma — Tel (6) 85 09
CCP 1/2640

Agencies
00187 Roma — Via del Tritone 61/A e 61/B
00187 Roma — Via XX Settembre (Palazzo Ministero delle finanze)
20121 Milano — Galleria Vittorio Emanuele 3
80121 Napoli — Via Chiaia 6
50129 Firenze — Via Cavour 46/R
16121 Genova — Via XII Ottobre 172
40125 Bologna — Strada Maggiore 23/A

NETHERLANDS

Staatsdrukkerij en uitgeverijbedrijf
Christoffel Plantijnstraat
's Gravenhage — Tel (070) 81 45 11
Giro 425 300

IRELAND

Stationery Office
Beggar's Bush
Dublin 4

SWITZERLAND

Librairie Payot
6 rue Grenus
1211 Genève
CCP 12 236 Genève

SWEDEN

Librairie C E Fritze
2, Fredsgatan
Stockholm 16
Post Giro 193, Bank Giro 73/4015

SPAIN

Librería Mundi Prensa
Castello 37
Madrid 1

OTHER COUNTRIES

Sales Office for official publications of the European Communities
Case postale 1003 — Luxembourg 1
Tel 4 79 41 — CCP 191-90
Compte courant bancaire, BIL 8-109/6003/200

OFFICE FOR OFFICIAL PUBLICATIONS OF THE EUROPEAN COMMUNITIES
Case postale 1003 — Luxembourg 1
5863